Supporting Information

Highly Efficient Top-Emitting Green Phosphorescent OLEDs with Narrow Band and Slow Efficiency Roll-off for High-Definition Displays

Jun Wang[a], Fanmin Meng[b], Weijian Liu[a], Zhaochao Zhang[c], Jiuyan Li[a*]

a Shandong Laboratory of Advanced Materials and Green Manufacturing at Yantai, Yantai Economic and Technological Development Zone, 300 Changjiang Road, Yantai, 264000, China. E-mail: greenjiuyanli@amgm.ac.cn (Jiuyan Li).

b Valiant Co., Ltd., No.11 Wuzhishan Road, YEDA, Yantai, Shandong Province, 264006, China.

c Jiangsu Sunera Technology Co., Ltd., Wuxi, 214028, China.

1. Experimental Section

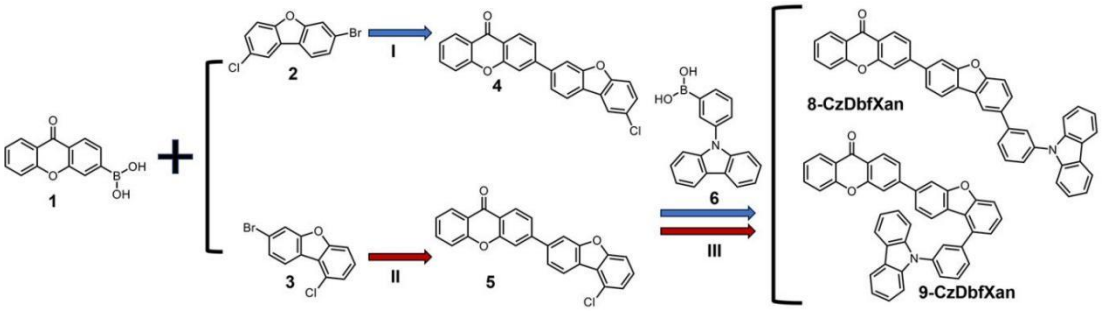

Scheme S1. Molecular structures and synthetic routes of 8-CzDbfXan and 9-CzDbfXan. Reaction condition: I, II: K_3CO_3, $Pd[P(PPh)_3]_4$, toluene/ethyl alcohol/H_2O, reflux, 15 h; III: K_2CO_3, $Pd[P(PPh)_3]_4$, toluene/ethyl alcohol/H_2O, reflux, 24 h.

1.1 General procedure for the synthesis of 8-CzDbfXan and 9-CzDbfXan

3-(8-chlorodibenzo[b,d]furan-3-yl)-9H-xanthen-9-one (compound 4) and 3-(9-chlorodibenzo[b,d]furan-3-yl)-9H-xanthen-9-one (compound 5) were synthesized according to the previously reported literature.[1] A mixture of compound 4 (1.0 eq, for 8-CzDbfXan) or compound 5 (1.0 eq, for 9-CzDbfXan), (3-(9H-carbazol-9-yl)phenyl)boronic acid (1.0 eq), K_2CO_3 (2.0 eq), $Pd(PPh_3)_4$ (0.02 eq) were dissolved in toluene/alcohol/H_2O and refluxed in N_2 atmosphere for 24 h. After cooling to RT, the mixture was extracted with CH_2Cl_2 and the organic phase was washed with acetonitrile-deionized water for 3 times. Then filter the organic phase under reduced pressure. The raw product was further purified by sublimation after performing column chromatography with silica gel to afford the pure 8-CzDbfXan

and 9-CzDbfXan.

8-CzDbfXan. White solid, 342 mg, yield 49%. ^{1}H NMR δ (400MHz, $CDCl_3$) 8.38 (t, 2H), 8.03 (d, 4H), 7.78 (d, 2H), 7.68-7.56 (m, 10H), 7.51 (t, 2H), 7.40 (d, 3H), 7.30 (s, 1H), 7.06 (s, 1H). ^{13}C NMR (126MHz, $CDCl_3$) δ 171.12, 156.77, 156.69, 148.08, 138.80, 135.17, 134.91, 132.02, 130.18, 129.31, 129.19, 129.11, 128.38, 127.45, 126.91, 126.76, 125.94, 125.45, 124.88, 124.12, 123.38, 123.34, 123.27, 123.05, 122.20, 120.52, 120.32, 119.80, 119.71, 118.10, 116.16, 112.20, 111.37, 110.02. HPLC-MS (*m/z*):604.29 [M^+].

9-CzDbfXan. white solid, 365 mg, yield, 52%. ^{1}H NMR δ (400MHz, $CDCl_3$) 8.35 (t, 2H), 8.17 (d, 2H), 7.82 (d, 2H), 7.79-7.65 (m, 2H), 7.70 (d, 4H), 7.51-7.39 (m, 9H), 7.38-7.26 (m, 4H). ^{13}C NMR (126 MHz, $CDCl_3$) δ 176.90, 157.21, 157.04, 156.55, 156.38, 147.32, 141.81, 138.55, 138.44, 136.91, 134.86, 130.23, 128.15, 127.77, 127.60, 127.45, 126.82, 126.16, 124.36, 124.16, 124.07, 123.65, 123.15, 122.70, 122.11, 122.07, 121.44, 120.84, 120.54, 120.25, 118.04, 116.15, 111.25, 110.52, 109.88. HPLC-MS (*m/z*):604.28 [M^+].

1.2 Materials and instruments

All our regents were used as received from commercial sources without further purification unless otherwise stated. The ^{1}H and ^{13}C nuclear magnetic resonance (NMR) spectra were measured on a Bruker Avance III 500 MHz NMR spectrometer. High-performance liquid chromatography-mass spectra (HPLC-MS) experiment was conducted on Thermo Fisher LCQ Fleet. UV-vis absorption spectra were recorded on a HP-8453 UV spectrophotometer. Photoluminescence (PL) spectroscopic studies

were performed on an Edinburgh FLS1000 fluorescence spectrometer. Differential scanning calorimetry (DSC) were determined on DSC-60 produced by Shimadzu. Thermogravimetric analysis (TGA) was conducted on TGA/DSC 3+ produced by METTLER TOLEDO. (Density functional theory) DFT and (time-dependent density functional theory) TD-DFT calculations were performance on Gaussian16 package at the B3LYP/6-31G(d) level. Ionization energy measurement was undertaken with an ionization potential spectrometer (Bunkoukeiki IPS-3). The root-mean-square-deviation (RMSD) values were computed using the VMD software after optimization. The electroluminescent (EL) properties at various viewing angles were evaluated on the FDS Optical Characteristics Automatic Testing System (FST Archina).

1.3 OLED fabrication and measurement

Glass substrates (50×50 mm) were cleaned in isopropanol using ultrasonic cleaner for 20 min after the pretreatment with detergent and deionized water, then dried in vacuum oven at 250 ℃ for 30 min and treated with oxygen plasma for 1 min. All organic and metal (Ag/Mg) materials were deposited layer by layer on the pre-cleaned glass substrates at the pressure below 1.33×10^{-4} Pa. The luminescent area was determined by anode and cathode overlapping as 2×2 mm. Finally, glass cover was applied to encapsulate devices. All the processes were carried out under N_2 atmosphere in glove box. The EL spectra of devices were measured on a PR-655 spectra scan spectrometer with computer control. The current-voltage-luminance characteristics were recorded by a system combined of the Keithley 2400 power

supply and a BM-7A luminance colorimeter. All the measurements were conducted at room temperature (RT) under ambient conditions.

2. Supplementary Figures and Tables.

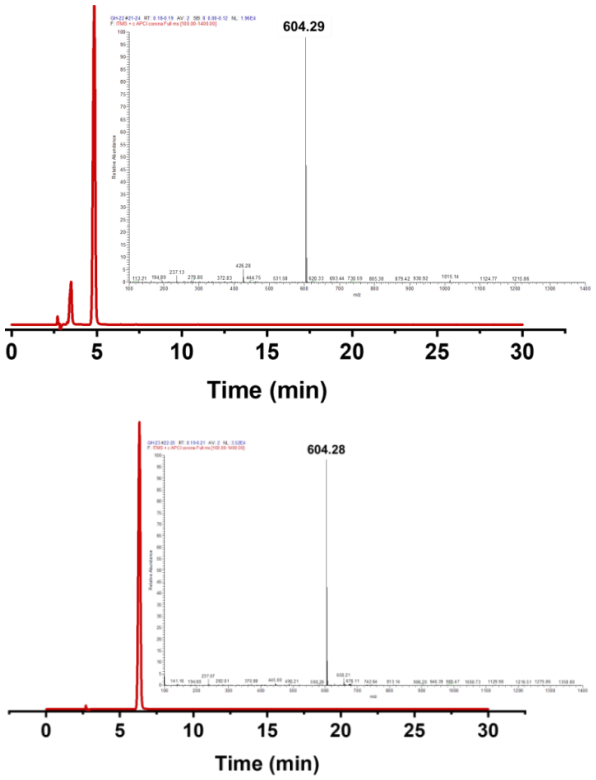

Fig. S1. The HPLC spectra of compounds 8-CzDbfXan (up) and 9-CzDbfXan (down) and their molecule weights obtained by HPLC-MS.

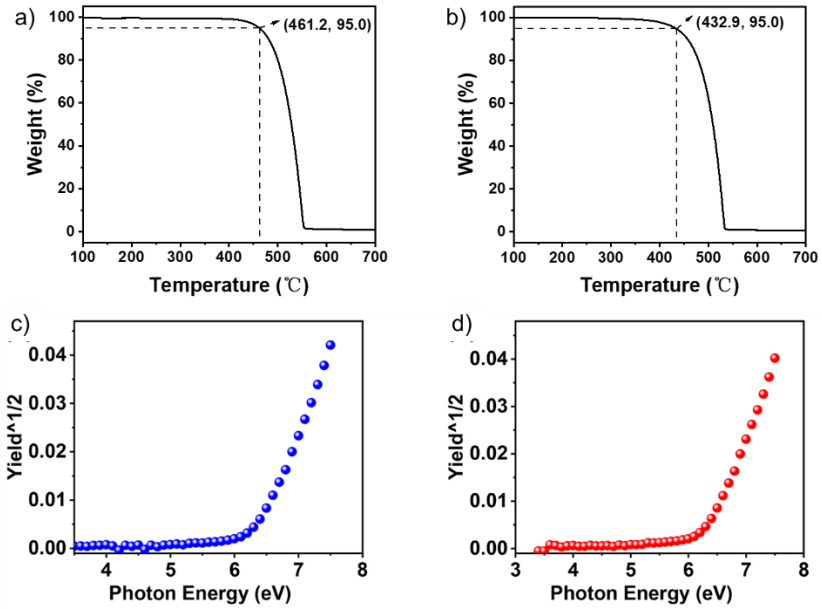

Fig.S2. The TGA curves (a, b) and the ionization energy spectra (c, d) of 8-CzDbfXan and 9-CzDbfXan.

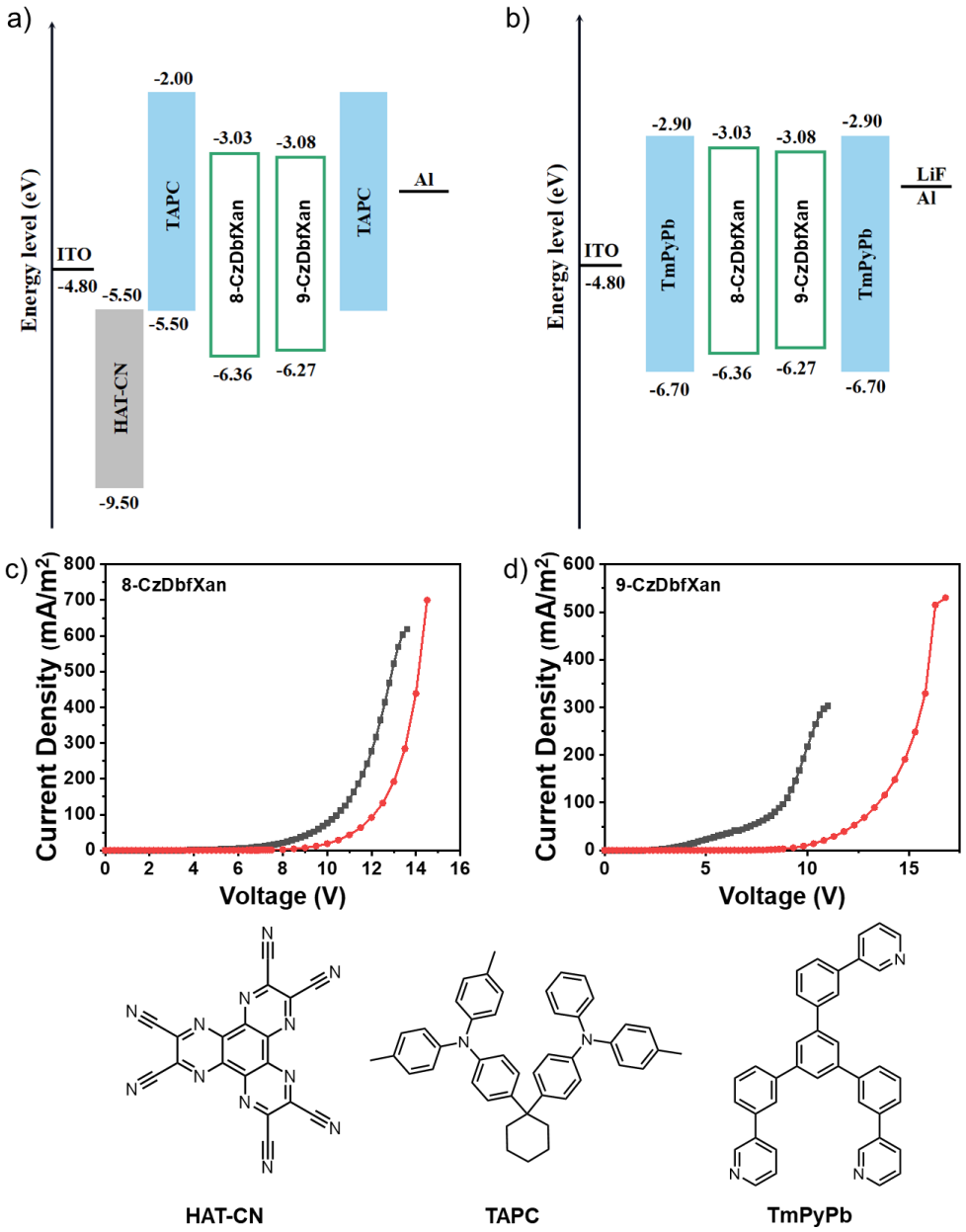

Fig.S3. Energy-level diagram of the single-carrier devices (a, hole-only device; b, electron-only device) containing the investigated host materials and the molecular structures of HAT-CN, TAPC and TmPyPb. Current density versus voltage curves of the electron-only (black) and hole-only (red) devices for 8-CzDbfXan (c) and 9-CzDbfXan (d).

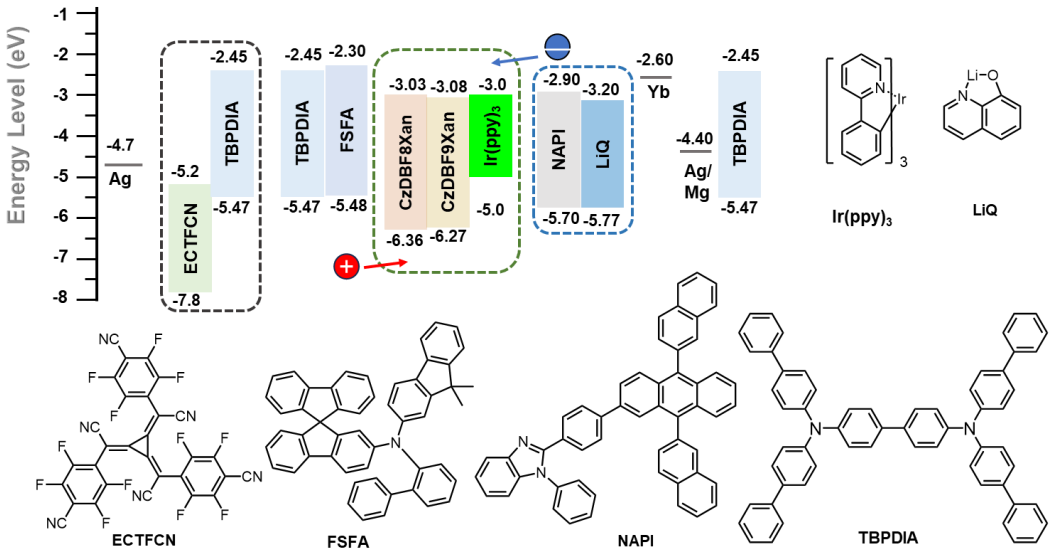

Fig. S4. Energy-level diagram of the top-emitting OLEDs containing the investigated host materials and the molecular structures of used materials.

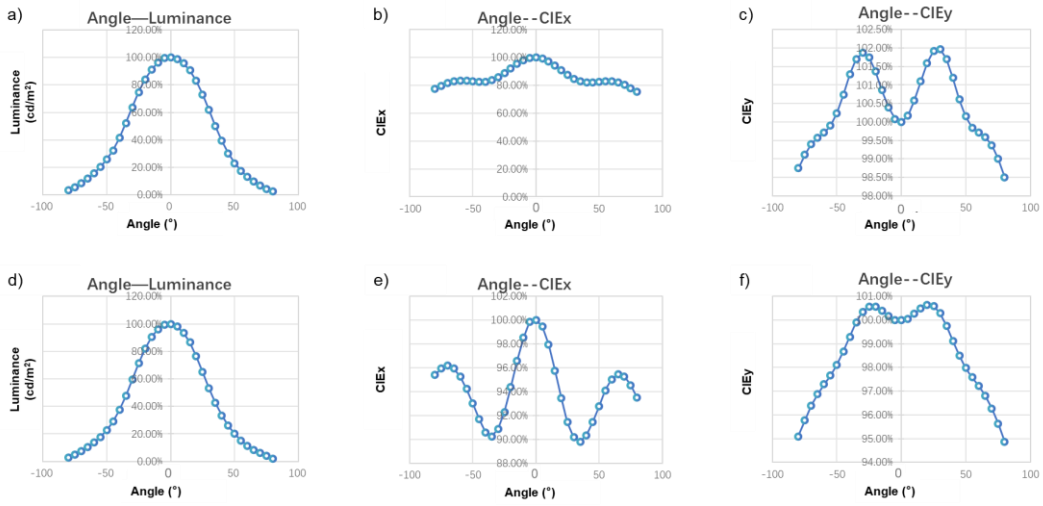

Fig. S5. Variation of the luminance, CIEx and CIEy at different view angles for the top-emitting devices A (a, b, c) and B (d, e, f), measured on FDS Optical Characteristics Automatic Testing System (FST Archina).

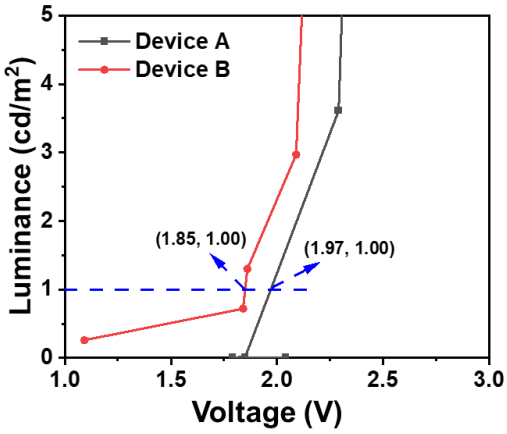

Fig. S6. Turn-on voltages of top-emitting devices A and B.

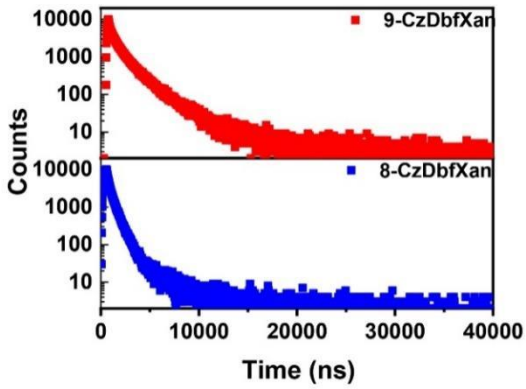

Fig. S7. Transient PL decay curves of the co-deposited 8-CzDbfXan:Ir(ppy)$_3$ and 9-CzDbfXan:Ir(ppy)$_3$ films.

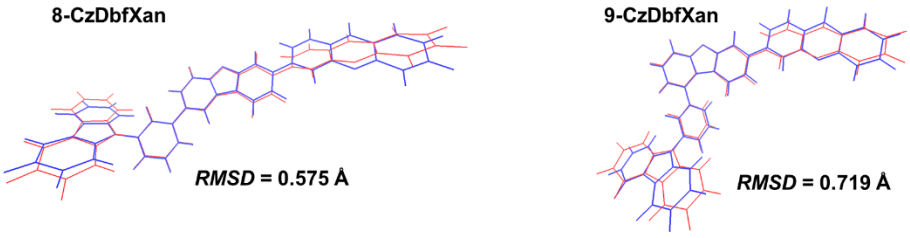

Fig. S8. The structural comparisons between S_0 (blue) and S_1 states (red) for 8-CzDbfXan and 9-CzDbfXan.

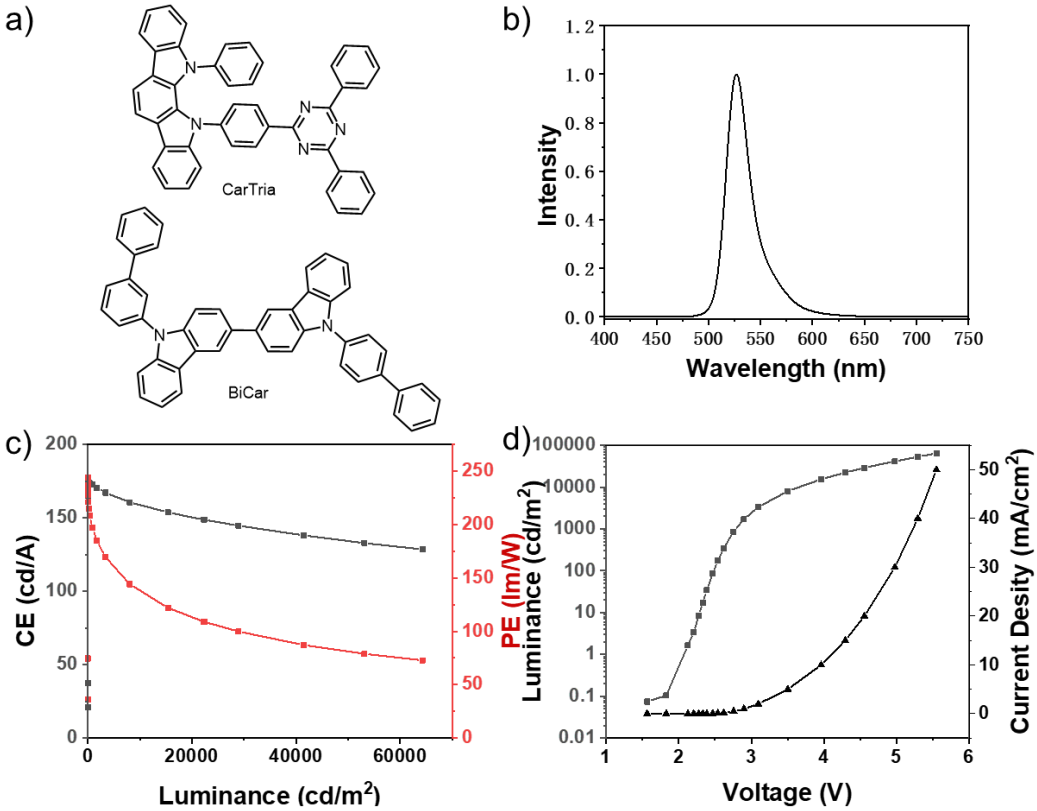

Fig. S9. The chemical structures (a) of commercial co-hosts (CarTria and BiCar) and EL performance (b, c and d) of the top-emitting OLED (device C) with the co-host.

Table S1. Electroluminescence properties of the device A.

Current density	**V**	**CE**	**PE**	**CIEx**	**CIEy**	**λpeak**	**L**	**FWHM**
(mA/cm^2)	(V)	(cd/A)	(lm/W)			(nm)	(cd/m^2)	
0.0002	2.04	3.36	5.17	0.2557	0.6758	527	0.0067	28.3
0.0005	1.79	1.80	3.16	0.2542	0.686	529	0.0090	28.6
0.0010	1.85	1.36	2.31	0.2525	0.6918	528	0.0136	28.8
0.0020	2.29	180.60	247.33	0.2487	0.7156	529	3.613	28.6
0.0050	2.35	182.25	243.14	0.248	0.7166	530	9.113	28.6
0.01	2.40	182.95	238.89	0.2473	0.7173	529	18.30	28.5
0.02	2.46	183.15	233.39	0.2466	0.7178	529	36.63	28.5
0.05	2.56	182.93	224.50	0.2457	0.7184	529	91.47	28.4
0.1	2.65	182.16	216.17	0.2451	0.7189	529	182.16	28.4
0.2	2.75	180.10	206.48	0.2445	0.7192	530	361.99	28.4
0.5	2.93	179.13	191.68	0.2435	0.7199	529	895.73	28.4
1	3.12	176.02	177.22	0.2431	0.7201	529	1760.2	28.4
2	3.37	171.69	160.14	0.2426	0.7203	529	3433.7	28.3
5	3.85	164.03	133.78	0.2422	0.7205	529	8201.8	28.4
10	4.37	156.57	112.49	0.2418	0.7207	529	15657	28.4
15	4.74	151.56	100.44	0.2417	0.7207	529	22735	28.5
20	5.02	147.56	92.21	0.2415	0.7207	528	29511	28.5
30	5.48	141.28	80.97	0.2414	0.7207	529	42381	28.6
40	5.81	136.33	73.63	0.2413	0.7206	529	54535	28.7
50	6.08	132.16	68.23	0.2414	0.7205	528	66085	28.8

Table S2. Electroluminescence properties of the device B.

Current density	**V**	**CE**	**PE**	**CIEx**	**CIEy**	**λpeak**	**L**	**FWHM**
(mA/cm^2)	(V)	(cd/A)	(lm/W)			(nm)	(cd/m^2)	
0.0002	1.092	131.31	377.61	0.2536	0.7131	531	0.26	28.3
0.0005	1.84	143.36	244.33	0.2523	0.7136	530	0.72	28.2
0.0010	1.86	129.65	218.46	0.2517	0.7148	530	1.30	28
0.0020	2.09	148.56	223.28	0.2507	0.7151	530	2.97	28
0.0050	2.15	150.07	219.36	0.2499	0.7163	530	7.50	28
0.01	2.19	150.29	215.11	0.2491	0.7172	530	15.02	27.9
0.02	2.24	150.23	210.28	0.2482	0.718	530	30.05	27.8
0.05	2.32	149.85	203.18	0.247	0.7189	530	74.93	27.7
0.1	2.38	149.04	196.84	0.2461	0.7194	530	149.04	27.7
0.2	2.45	148.21	190.07	0.2452	0.7201	530	296.42	27.7
0.5	2.57	146.01	178.58	0.2441	0.7207	530	730.09	27.7
1	2.69	143.96	168.18	0.2429	0.7215	530	1439.6	27.7
2	2.85	139.90	154.08	0.242	0.7221	529	2798	27.7
5	3.18	131.92	130.25	0.2408	0.7229	529	6596.2	27.7
10	3.56	123.38	108.96	0.2398	0.7234	529	12338	27.6
15	3.83	117.16	96.01	0.2393	0.7238	529	17575	27.6
20	4.05	112.17	86.90	0.2389	0.724	529	22435	27.6
30	4.41	104.16	74.16	0.2383	0.7243	529	31245	27.7
40	4.68	97.99	65.71	0.2379	0.7246	529	39199	27.7
50	4.91	92.89	59.43	0.2376	0.7246	529	46449	27.7

Table S3. Summary of device performance of the representative top-emitting green PhOLEDs reported during the last decade.

EML	PE_{max} (lm/W)	CE_{max} (cd/A)	FWHM (nm)	CIE	Ref.
8-CzDbfXan/Ir(ppy)$_3$	**247.3**	**183.1**	**28.4**	**(0.243, 0.720)**	**This work**
9-CzDbfXan/Ir(ppy)$_3$	**244.3**	**150.3**	**27.7**	**(0.241, 0.722)**	**This work**
CarTria & Bicar /Ir(ppy)$_3$	244.2	173.8	26.7	(0.227, 0.729)	This work
GHA1/Ir(ppy)$_3$	283.3	190.8	31.7	(0.25, 0.71)	[1]
GHA2/Ir(ppy)$_3$	245.2	169.0	28.4	(0.23, 0.73)	[1]
GHA3/Ir(ppy)$_3$	225.3	166.4	27.1	(0.22, 0.73)	[1]
GHA4/Ir(ppy)$_3$	247.5	181.8	28.3	(0.22, 0.73)	[1]
BN-ICz-1/mCBP /Ir(ppy)$_2$acac	/	220	19	(0.17, 0.78)	[2]
TCTA/Ir(mppy)$_3$	/	161.2	20	/	[3]
Bepp$_2$/ Ir(ppy)$_3$	95.2	93.7	31	/	[4]
CBP/PtN7N	71.0	98.8	21	(0.18, 0.74)	[5]
CBP/Ir(mppy)$_3$	35.7	64	23	(0.236, 0.728)	[6]
Bepp$_2$/ Ir(ppy)$_2$acac	/	167.2	29	(0.224, 0.736)	[7]
TmPPPyTz:Ir(ppy)$_3$	55.2	56.2	/	/	[8]
CBP/Ir(ppy)$_2$acac	~180	/	/	/	[9]
CBP/Ir(ppy)$_2$acac	290[a]	/	62	(0.28, 0.66)	[9]
CBP/Ir(ppy)$_3$	/	69	/	/	[10]

[a]with lens-based structure on the device.

Table S4. Summary of quantum yield (Φ_{PL}), phosphorescence lifetimes (τ), radiative and non-radiative rate constants (K_r and K_{nr}) of the co-deposited films of $Ir(ppy)_3$ in 8-CzDbfXan and 9-CzDbfXan.

Material	τ (μs)	Φ_{PL}	K_{nr}	K_r	K_r/K_{nr}
8-CzDbfXan	6.4	99.3	9.4×10^2	1.5×10^5	159.6
9-CzDbfXan	27.7	98.5	5.4×10^2	3.6×10^4	66.7

Table S5. Electroluminescence properties of the control device C.

Current density	**V**	**CE**	**PE**	**CIEx**	**CIEy**	**λpeak**	**L**	**FWHM**
(mA/cm²)	(V)	(cd/A)	(lm/W)			(nm)	(cd/m²)	
0.0002	1.57	37.13	74.4454	0.2377	0.7191	527	0.0741	27.1
0.0005	1.83	20.94	35.9554	0.2377	0.7195	527	0.1047	27.2
0.0010	2.13	165.30	244.2091	0.2351	0.7232	528	1.653	27.1
0.0020	2.21	168.08	239.3476	0.2349	0.7232	528	3.3624	27.1
0.0050	2.28	170.69	235.4562	0.2342	0.7244	527	8.5353	27.1
0.01	2.33	172.10	231.9058	0.2335	0.7251	527	17.21	27
0.02	2.39	173.09	227.7664	0.2327	0.7257	527	34.619	27
0.05	2.47	173.81	221.1887	0.2318	0.7264	527	86.914	26.9
0.1	2.54	173.82	215.1226	0.231	0.7269	527	173.82	26.9
0.2	2.62	173.52	208.0787	0.2302	0.7274	527	347.04	26.9
0.5	2.76	172.73	196.8149	0.229	0.7281	527	863.7	26.9
1	2.90	170.50	184.7953	0.2283	0.7285	527	1705.1	26.8
2	3.10	167.13	169.582	0.2278	0.7289	527	3342.6	26.8
5	3.50	160.62	144.0552	0.2271	0.7292	527	8031.5	26.7
10	3.96	153.75	121.9276	0.2266	0.7294	527	15375	26.8
15	4.29	148.72	108.8145	0.2264	0.7294	527	22309	26.7
20	4.56	144.69	99.7536	0.2262	0.7294	527	28938	26.8
30	4.98	138.08	87.1629	0.226	0.7294	526	41422	26.8
40	5.29	132.83	78.842	0.2259	0.7295	526	53133	26.8
50	5.55	128.53	72.7719	0.2259	0.7293	526	64267	26.9

Reference

[1] Li, L., Wang, H., Cao, X., Xu, K., Zhu, S., Liu, R., Song, G. High-Efficiency Green Organic Light-Emitting Devices with Low Efficiency Roll-Off Using π-Shape Materials as Host. Org. Electron., 2023; 120, 106856.

[2] Zhang, Y., Li, G., Wang, L., Huang, T., Wei, J., Meng, G., Duan, L. Fusion of Multi-Resonance Fragment with Conventional Polycyclic Aromatic Hydrocarbon for Nearly Bt.2020 Green Emission. Angew. Chem. Int. Ed., 2022; 61, e202202380.

[3] Li, X., Liu, W., Chen, K., Wu, R., Liu, G. & Zhou, L. High-Performance Narrow Spectrum Green Phosphorescent Top-Emitting Organic Light-Emitting Devices with External Quantum Efficiency up to 38%. Semicond. Sci. Technol., 2022; 37, 015016.

[4] Park, M. J., Son, Y. H., Kim, G. H., Lampande, R., Bae, H. W., Pode, R., Kwon, J. H. Device Performances of Third Order Micro-Cavity Green Top-Emitting Organic Light Emitting Diodes. Org. Electron., 2015; 26, 458-463.

[5] Fukagawa, H., Oono, T., Iwasaki, Y., Hatakeyama, T. & Shimizu, T. High-Efficiency Ultrapure Green Organic Light-Emitting Diodes. Mater. Chem. Front., 2018; 2, 704-709.

[6] Kim, J. Y., Lee, S. Y., Cho, K. H. & Do, Y. S. Dual-Microcavity Technology for Red, Green, and Blue Electroluminescent Devices. Adv. Funct. Mater., 2023, 33, 2305528.

[7] Kim, S. K., Lampande, R. & Kwon, J. H. Electro-Optically Efficient and Thermally Stable Multilayer Semitransparent Pristine Ag Cathode Structure for Top-Emission Organic Light-Emitting Diodes. Acs Photonics, 2019; 6, 2957-2965.

[8] Wu, Y., Zhang, Z., Yue, S., Huang, R., Du, H. & Zhao, Y. High Performance Top-Emitting Organic Light-Emitting Diodes for Super Video Graphics Array Monochromatic Microdisplays Application. Chin. J. Chem., 2015; 33, 897-901.

[9] Wang, Z. B., Helander, M. G., Qiu, J., Puzzo, D. P., Greiner, M. T., Hudson, Z. M., Lu, Z. H. Unlocking the Full Potential of Organic Light-Emitting Diodes on Flexible Plastic. Nat. Photonics, 2011; 5, 753-757.

[10] J-H Lee; D-S Leem; J-J Kim. High performance top-emitting organic light-emitting diodes with copper iodide-doped hole injection layer. Org. Electron, 2008; 9, 805–808